

Microscopic interactions control a structural transition in active mixtures of microtubules and molecular motors

Bibi Najma^a, Wei-Shao Wei^a, Aparna Baskaran^a, Peter J. Foster^{a,1}, and Guillaume Duclos^{a,2}

Edited by Martin Lenz, Universite Paris-Saclay, Orsay, France; received January 4, 2023; accepted October 7, 2023 by Editorial Board Member Daan Frenkel

Microtubules and molecular motors are essential components of the cellular cytoskeleton, driving fundamental processes in vivo, including chromosome segregation and cargo transport. When reconstituted in vitro, these cytoskeletal proteins serve as energy-consuming building blocks to study the self-organization of active matter. Cytoskeletal active gels display rich emergent dynamics, including extensile flows, locally contractile asters, and bulk contraction. However, it is unclear how the protein-protein interaction kinetics set their contractile or extensile nature. Here, we explore the origin of the transition from extensile bundles to contractile asters in a minimal reconstituted system composed of stabilized microtubules, depletant, adenosine 5'-triphosphate (ATP), and clusters of kinesin-1 motors. We show that the microtubule-binding and unbinding kinetics of highly processive motor clusters set their ability to end-accumulate, which can drive polarity sorting of the microtubules and aster formation. We further demonstrate that the microscopic time scale of end-accumulation sets the emergent time scale of aster formation. Finally, we show that biochemical regulation is insufficient to fully explain the transition as generic aligning interactions through depletion, cross-linking, or excluded volume interactions can drive bundle formation despite end-accumulating motors. The extensile-to-contractile transition is well captured by a simple self-assembly model where nematic and polar aligning interactions compete to form either bundles or asters. Starting from a five-dimensional organization phase space, we identify a single control parameter given by the ratio of the different component concentrations that dictates the material-scale organization. Overall, this work shows that the interplay of biochemical and mechanical tuning at the microscopic level controls the robust self-organization of active cytoskeletal materials.

active matter | molecular motors | microtubules | self-organization

Active materials are far-from-equilibrium materials composed of energy-consuming building blocks (1). They self-organize into spontaneously moving structures larger than their microscopic components, and their material-scale mechanics emerge from nonequilibrium interactions between active units. In thermodynamically driven self-assembly, the emergent structures are set by the interaction strengths of the various molecules (2). In active materials, pattern formation often results from dynamical processes whose characteristic time scale sets the emergent structure and dynamics (3).

Many examples of in vitro cytoskeletal materials self-organize into distinct states, which reflect the richness of the microscopic interactions between various molecular motors and cytoskeletal filaments. In particular, these materials often display bulk extensile (4-6) or contractile and aster-forming behaviors (7-18). Extensile dynamics have been associated with active systems organized into mesoscopic polymer bundles, frequently through the addition of a depletion agent. Such extensile flows have been reported for both microtubule/ kinesin (4, 6, 18) and actomyosin (19, 20) based materials. Theoretical work has suggested that extensile stresses could arise from the polarity sorting of filaments (21) or the mechanical properties of the motors themselves (22, 23). In the absence of depletant, both microtubule and actin-based active gels can undergo bulk contraction. However, the mechanisms that lead to extensile or contractile dynamics might differ as actin and microtubules have very different mechanical properties. Actomyosin contraction is also fundamentally rooted in symmetry-breaking at the filament level, either because of the nonlinear mechanical properties of actin filaments (11, 24-26), end-accumulation of myosin motors (16, 27), or through the asymmetric distribution of cross-linkers or motor proteins (28). Microtubule bulk contraction has been argued to stem from contractile active stresses generated by the clustering of microtubule ends by end-accumulating motors (7, 12, 29, 30).

While dyneins and many kinesins are known to end-accumulate (31–34), many motors including dimeric kinesin-1—have been argued not to under physiological conditions because of their low processivity (<1 µm (35)), even on stabilized microtubules (32, 35,

Significance

Self-organization in living cells is often driven by energyconsuming motor proteins that push and pull on a network of cytoskeletal filaments. However, it is unclear how to connect the emergent structure and dynamics of reconstituted cytoskeletal materials to the kinetics and mechanics of their microscopic building blocks. Here, we systematically correlate bulk structure with asymmetry of the motor distribution along single filaments to explain the transition from extensile bundles to contractile asters in active networks of stabilized microtubules cross-linked by motor proteins. We combine experiments and scaling arguments to identify a single parameter that predicts how the system will self-organize at steady state. This work shows that biochemical and mechanical interactions compete to set the emergent structure of active materials.

Author contributions: B.N., P.J.F., and G.D. designed research; B.N. performed research; B.N., W.-S.W., A.B., P.J.F., and G.D. contributed new reagents/analytic tools; B.N., W.-S.W., P.J.F., and G.D. analyzed data; and B.N., P.J.F., and G.D. wrote the paper.

The authors declare no competing interest.

This article is a PNAS Direct Submission. M.L. is a guest editor invited by the Editorial Board.

Copyright © 2024 the Author(s). Published by PNAS. This article is distributed under Creative Commons Attribution-NonCommercial-NoDerivatives License 4.0

¹Present address: Department of Physics and Astronomy, Bridge Institute, Michelson Center for Convergent Bioscience, University of Southern California, Los Angeles, CA 90089.

²To whom correspondence may be addressed. Email: gduclos@brandeis.edu.

This article contains supporting information online at https://www.pnas.org/lookup/suppl/doi:10.1073/pnas. 2300174121/-/DCSupplemental.

Published January 4, 2024.

36). Indeed, theory and experiments demonstrated that the processivity, binding, and unbinding kinetics are crucial in determining whether molecular motors will end-accumulate on isolated stabilized microtubules (32, 37). Furthermore, the motor binding and unbinding kinetics depends on several factors, including salt concentration and the concentrations of motors and adenosine 5'-triphosphate (ATP). Increasing ATP concentration leads to a higher dissociation rate (38) and increased motor speed (39), which saturate at high ATP concentration. Finally, as processivity increases when motors can bind to multiple sites along a single filament (40), the multivalency of the motors is important to consider as many motors form clusters, either naturally or by design (4, 7, 19, 41). Thus, whether or not a motor will end-accumulate is determined in part by the motor's environment.

On the theoretical front, simple theories and simulations have addressed the origin of contractility in cross-linked networks composed of rigid or semiflexible polymers and molecular motors (25, 30, 42), highlighting the importance of having passive cross-linkers that create an elastically percolated network. For end-accumulating motors, experiments and computer simulations showed that the competition between motor cross-linking either the ends or the sides of microtubules sets the extensile or contractile dynamics of the active network (43). However, despite these advances, the rational design of a simple and programmable biomimetic material that could exert both extensile and contractile stresses is still challenging. Recent in vitro experiments and simulations show that microtubule networks composed of a mixture of motors with opposite directionality can display either extensile or contractile dynamics depending on the relative concentration of each motor protein (43, 44). In the presence of a single type of end-accumulating motor, competition between microtubule growth rate and motor speed dictates if bulk dynamics are extensile or contractile (43).

Most reconstituted active systems are composed of stabilized microtubules and a single type of motor, and were thought to display a single bulk organization—either contractile or extensile (4, 7, 12). However, two recent examples, with clusters of kinesin-1 motors (18, 45) and end-accumulating kinesin-4 motors (34), show that networks of stabilized microtubules cross-linked by a single type of motor proteins can display both extensile and contractile dynamics. The underlying physical or biochemical mechanisms that lead to this phenomenon are unclear. In particular, the role of motor-microtubule interaction kinetics in determining the emergent structure of the active microtubule-kinesin gel is unknown. There is, therefore, a need for a careful study of the simplest system possible, with stabilized microtubules and a single motor type, to uncover the microscopic origin of the extensile-to-contractile transition.

Here, we assembled an active gel composed of stabilized microtubules, a bundler, and kinesin-1 motor clusters. We systematically combined bulk experiments with direct observation at the single filament level to study how emergent bulk dynamics is related to the distribution of processive motor clusters along microtubules. Extensile flows emerged when the motors were uniformly distributed and the active gel contracted when motors end-accumulated. We show that end-accumulation and contraction can be induced by either increasing motor cluster concentration or decreasing ATP concentration, which is consistent with increasing the lattice-binding rate and decreasing the lattice-dissociation rate of the motor-microtubule binding kinetics. Our study goes beyond steady-state dynamics, showing that the microscopic timescale of end-accumulation and the macroscopic timescale for aster formation are correlated. Finally, increasing nematic alignment by adding either a nonspecific depletant, a microtubule-specific cross-linker, or colloidal rods, triggers the reversed transition from asters to bundles without impacting motor cluster end-accumulation at the single filament level. A simple self-assembly model at steady-state demonstrates that the bundle-aster phase boundary results from the competition between polar sorting and nematic alignment. This model allows us to predict the emergent structure based on a single control parameter given by the ratio of the various component concentrations.

Results

Our minimal in vitro system is composed of microtubules and multivalent clusters of molecular motors (Fig. 1A) (4, 46). Guanosine-5'- $[(\alpha, \beta)$ methyleno]triphosphate (GMPCPP)-stabilized microtubules are bundled by a nonspecific depletant (20 kDa Poly(ethylene glycol) PEG). Individual motor clusters are composed of four kinesin dimers bound to one tetravalent streptavidin, a lower-bound average composition inferred from dynamic light scattering measurements (Fig. 1B and SI Appendix, Fig. S1 and section 2b). Each kinesin dimer is composed of two biotinylated truncated kinesin-1 motors (consisting of the first 401 amino acids of kinesin-1) that spontaneously dimerize to form a processive double-headed motor. These motor clusters can simultaneously bind to multiple microtubules, taking steps upon hydrolysis of ATP. This cross-linking and walking motion results in the sliding of adjacent antiparallel microtubules. In this configuration, a microtubule bundle continuously elongates over time, exerting dipolar extensile stresses (4, 6, 47). Microtubule bundles form a continuously reconfiguring three-dimensional active gel that powers autonomous extensile flows (4, 48) (Fig. 1C and Movie S1). In this extensile phase, dual-color imaging of microtubules and motor clusters revealed a uniform distribution of the motors along the microtubule bundles (Fig. 1 F and G and SI Appendix, Fig. S2 A–C).

Assembling active gels with increasing motor cluster concentrations led to a radical change in the emergent structure and dynamics of the active gels: Above a critical motor cluster concentration, the active network transitioned from forming an extensile phase into forming a contractile phase, where large microtubule asters coexist with an extensile background (Fig. 1D and Movie S2). Dual-color imaging of microtubules and kinesin-1 clusters revealed that the aster cores were enriched with motor clusters (Fig. 1 H and I and SI Appendix, Fig. S2 D-F), a generic feature of both actin-based (16, 27) and microtubule-based asters, both in vitro (18, 34, 43, 49) and in cellular extracts (12, 50-52). Further increasing the motor cluster concentration led to a second transition from a locally contractile aster phase to a globally contractile phase (Fig. 1*E* and Movie S3).

We further investigated how the binding and unbinding rates of kinesin onto microtubules control the macroscopic organization of the network by changing the concentrations of ATP and motor clusters while keeping the microtubules' length and the concentrations of microtubules and PEG constant. The resulting phase diagram reveals that the critical motor cluster concentration that triggers aster formation depends on the ATP concentration (Fig. 1/). Asters displayed enrichment of motors in their core (Fig. 1I and SI Appendix, Fig. S2 D-F), a hallmark of asymmetric motor distribution. Hence, we hypothesized that modulating the ATP and kinesin concentrations changes the degree of motor end-accumulation, and hence the system's propensity toward contractility.

To test this hypothesis, we looked at the distribution of fluorescent motor clusters along isolated microtubules (Fig. 2A and SI Appendix, section 2a). We observed that motor clusters were uniformly distributed along microtubules in conditions where the gel was extensile (Fig. 2 C and F). However, when the concentration of ATP was decreased (Fig. 2 B and D) or the concentration

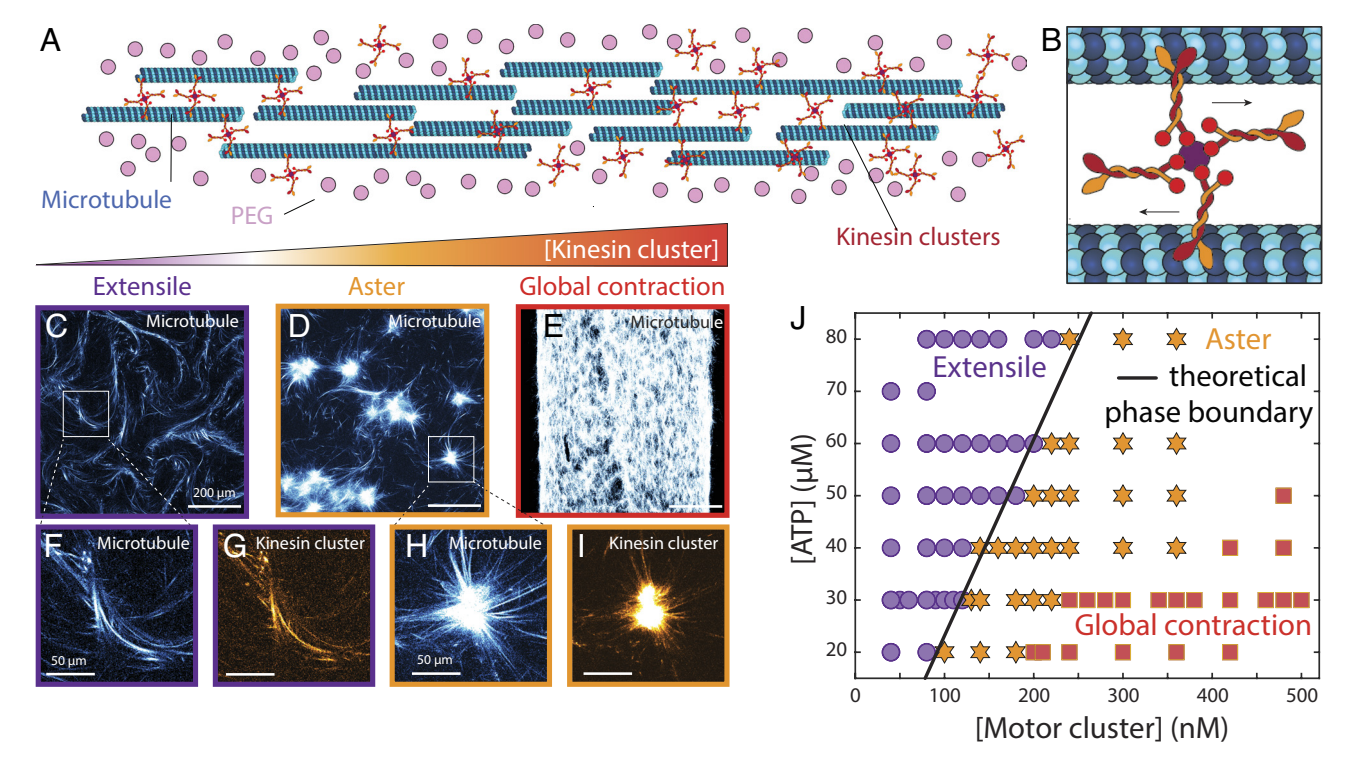


Fig. 1. Multivalent clusters of kinesin-1 molecular motor drive microtubule gels into extensile, aster, or globally contractile phases. (A) Schematic of an extensile bundle of stabilized microtubules. (B) Close up on a single multivalent motor cluster—four kinesin-1 dimers bound to one tetravalent streptavidin—walking toward the plus end of the microtubules. (C) Fluorescent picture of the microtubule gel in the extensile phase ([motor clusters] = 60 nM). Increasing the cluster concentration first leads to the formation of (D) an aster phase that locally contracts ([motor clusters] = 120 nM) and then (E) a globally contractile phase ([motor clusters] = 480 nM). (F and G) show close-ups of fluorescently labeled tubulin and motor clusters for an extensile bundle. (H and I) show close-ups of fluorescently labeled tubulin and motor clusters for an aster. (/) ATP-motor cluster phase diagram: the critical concentration of motors needed to form asters and contract depends on the ATP concentration. Purple disks represent extensile bundles, orange stars are asters, and red squares are globally contractile gels. Each data point is an independent experiment. (C-I) were taken with a confocal microscope. Scale bars in (C-E) are 200 μm. Scale bars in (F-I) are 50 μm. In (C-J), [ATP] = $30 \mu M$, [PEG] = 0.6% vol/vol, [tubulin] = 1.33 mg/mL.

of motor clusters was increased (Fig. 2 G and H), motor clusters formed dense aggregates on one end of the microtubules and the corresponding bulk dynamics were contractile. We confirmed these trends by quantifying the fraction of microtubules with motor cluster caps for a wide range of ATP and motor cluster concentrations (SI Appendix, section 4a). Decreasing ATP concentration or increasing motor cluster concentration led to an increase in the fraction of microtubules with motor caps (Fig. 2 *E* and *I*). Interestingly, we report that the probability of having a cap increased with microtubule length (SI Appendix, Fig. S3E). Hence, an antenna model may underlie the cap formation process: More motors can be captured by longer microtubules, resulting in a higher probability to form a motor cap (32, 53). We tested the impact of microtubule length on the macroscale organization by annealing microtubules while fixing the tubulin concentration: Microtubules got longer while their number density decreased. This led to a transition from extensile bundles to contractile asters (SI Appendix, Fig. S3 A-D). Decreasing microtubule density while keeping their average length constant also led to a transition from extensile to contractile dynamics (*SI Appendix*, Fig. S4A).

Inspired by experiments and theory describing the mechanisms that underlie end-accumulation of highly processive Kip3 motors on microtubules (32), we hypothesized that the processivity of the motor clusters is a key feature that enables the formation of caps and the assembly of contractile asters. Dimeric Kinesin-1 motors have a run length of less than 1 µm (35). Here, we measured a lower bound for the run length of K401 motor clusters under conditions where they end-accumulate and found an average minimal run length of $5.7 \pm 2.6 \mu m$ (N = 216 runs, SI Appendix, Fig. S5 A and B), while the mode of the microtubule length

distribution was around 1.6 µm (N > 6,000 microtubules, SI Appendix, Fig. S5C). To further confirm the importance of high processivity, we increased the dissociation rate of the motor clusters by increasing the salt concentration. We observed a transition from contractile to extensile bulk dynamics (SI Appendix, Fig. S6 A, B, E, and F). Additionally, motor clusters were found to not end-accumulate when salt concentration was increased, consistently with a higher dissociation rate (SI Appendix, Fig. S6 C, D, *G*, and *H*).

To confirm that motor cluster processivity is required for endaccumulation, we leveraged a recently developed light-dimerizable K365 kinesin-1 motor protein (first 365 amino acids of Kinesin-1) (54). Contrary to the processive dimeric K401 protein, this monomeric derivative of kinesin-1 is nonprocessive: Motors detach from microtubules after each step (55). Each motor presents either an iLid or a microtag which dimerize when exposed to blue light (15, 56) (SI Appendix, Fig. S7A). Native gel experiments demonstrated that equimolar mixtures of these two motors do not spontaneously dimerize when not exposed to blue light (SI Appendix, Fig. S7 B and C). Further, as these motor clusters do not contain streptavidin linkers, the valency of the clusters is limited by design to two single-headed nonprocessive motors. Here, we performed bulk experiments in the absence of depletant to test the ability of these motor dimers to form asters. We combined stabilized microtubules with an equimolar mixture of iLid and micro-K365 motors and continuously exposed the sample to blue light while imaging the bulk dynamics. ATP concentrations were varied from 5 to 100 μM, and motor concentrations were varied from 100 to 500 nM. While all the other kinesin-1 clusters tested assembled microtubules into asters [including light-dimerizable iLid/micro

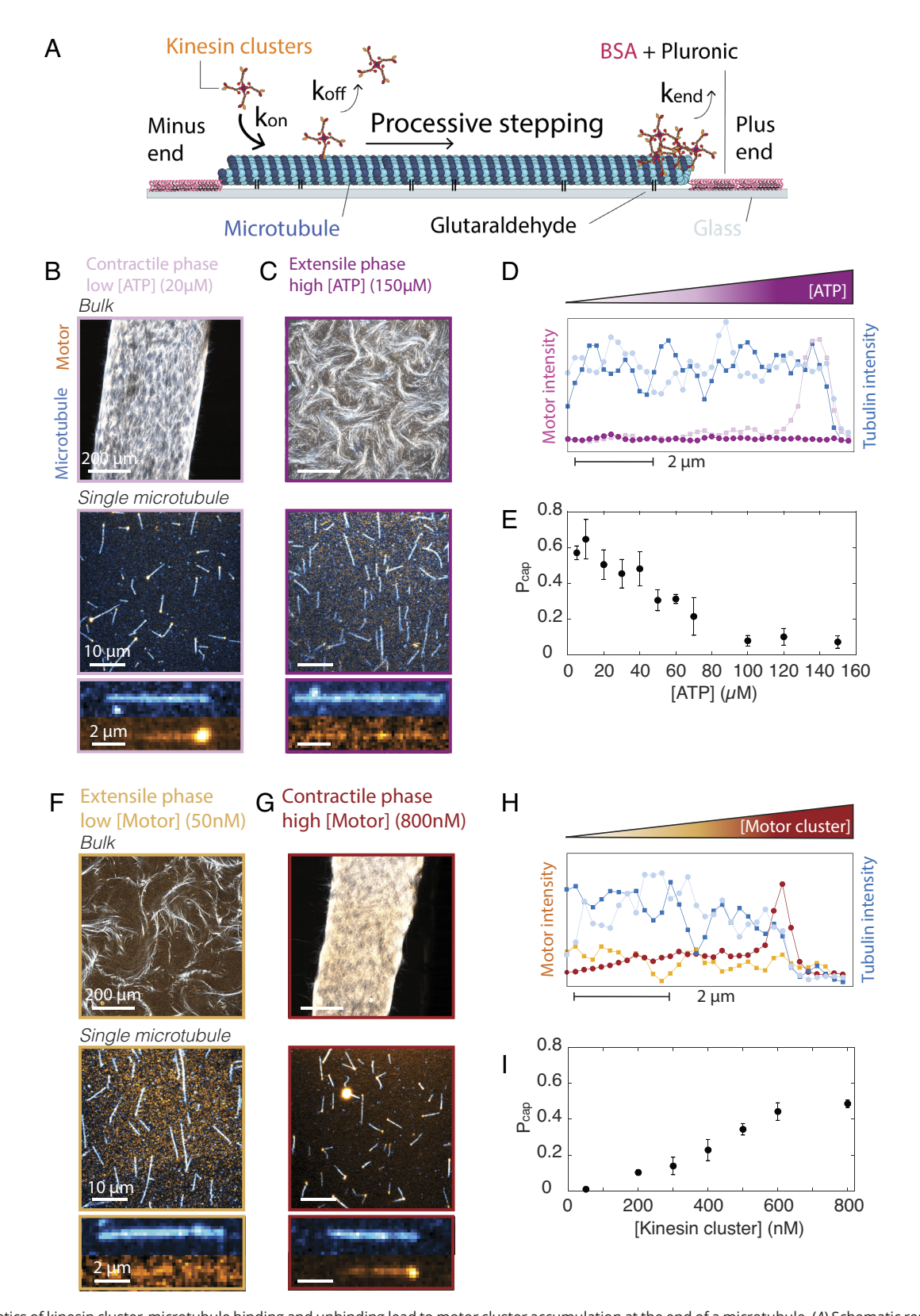


Fig. 2. Kinetics of kinesin cluster-microtubule binding and unbinding lead to motor cluster accumulation at the end of a microtubule. (A) Schematic representation of the microscopic interaction between a microtubule and multivalent motor clusters. (B and C) Fluorescent pictures of bulk active gels and corresponding fluorescent pictures of isolated microtubules bound to a glass surface at low and high ATP concentrations. (D) Line scans of the fluorescent intensity along a single microtubule for the pictures shown in (B) and (C). Microtubule profiles are in cyan, and motor cluster profiles are in magenta. (E) Fraction of microtubules with a motor cluster cap for increasing ATP concentrations. (F and G) Fluorescent pictures of bulk active gels and corresponding fluorescent pictures of isolated microtubules bound to a glass surface at low and high motor cluster concentrations. (H) Line scans of the fluorescent intensity along a single microtubule for the pictures shown in (F) and (G). Microtubule profiles are in cyan, and motor cluster profiles are in orange. (I) Fraction of microtubules with a motor cluster cap for increasing motor cluster concentrations. In (B and C) and (F and G), Tubulin is labeled in cyan, and motor clusters are in orange. For (B-E), [motor cluster] = 480 nM; for (F-I), [ATP] = 30 μM.

clusters of processive K401 (15)], we never observed the formation of asters with iLid/micro-K365 motor dimers (SI Appendix, Fig. S7D). Assembling active microtubule gels with iLid/micro dimers of nonprocessive K365 and a depletant (20 kDa PEG) recovered the extensile dynamics previously reported for this light-activable active gel (SI Appendix, Fig. S7D) (54).

To further examine the causal link between motor cluster end-accumulation and the formation of contractile asters, we compared the dynamics of both processes (Fig. 3). Close to the contractile-to-extensile phase boundary, asters did not appear instantaneously (Fig. 3A). Rather, active gels first displayed extensile dynamics before one or more asters nucleated (Fig. 3A). We systematically measured the time evolution of aster density and found that increasing ATP concentrations delayed asters nucleation (Fig. 3B). Similarly, at the microscopic scale, we found that motor caps formed at slower rates when ATP concentration was increased (Fig. 3 C and D). We independently measured the time at which the first aster nucleates and the time at which 10% of the microtubules have motor caps under identical buffer conditions. Comparing the two characteristic timescales showed that the dynamics of motor cap and aster formations were correlated (Fig. 3E). This analysis provides direct evidence that the microscopic timescale set the emergent timescale.

Taken together, these experiments demonstrate that both the steady-state organization and the dynamics of the self-organization at the macroscopic scale are controlled by the kinetics at the microscopic scale. The microtubule binding and unbinding kinetics of processive motor clusters dictate if and when motors will start to end-accumulate, which is necessary to trigger the transition from extensile bundles to contractile asters. The binding rate of kinesin clusters, k_{on}, has been shown to increase when the concentration of motor clusters increases, and the dissociation rate, k_{off}, decreases when ATP concentration decreases (38). Both mechanisms favor the end-accumulation of highly processive motors (32), which, in our case, also triggers end-clustering of the microtubules and aster formation at the macroscopic scale.

However, considering the binding kinetics between motors and microtubules is insufficient to explain fully how kinesin-microtubule networks self-organize in the presence of crowding agents or cross-linkers. Indeed, adding a depletant such as PEG transformed a contractile phase into an extensile phase without impacting the ability of the motor clusters to end-accumulate at the single filament level (Fig. 4 A, B, E, and F). An extensive PEG-motor cluster phase diagram suggests that the contractile-extensile phase boundary results from a competition between the ability to form polar motor caps and the depletion force (Fig. 4/). Indeed depletion promotes nematic alignment of microtubules into bundles (57), while motor cluster caps promote polar sorting and aster formation (43). We explored how other mechanisms that induce nematic alignment impact the emergent bulk dynamics. We first showed that adding PRC1, a cross-linking protein that binds diffusively to microtubules (58–60), also converted a contractile phase into an extensile phase (Fig. 4C). Starting from a globally contractile phase, adding cross-linkers first led to the formation of the aster phase and then an extensile phase (SI Appendix, Fig. S8). Second, we enhanced the nematic alignment of the microtubules by adding passive semiflexible polymers—either filamentous *fd* viruses (61) or DNA-origami rods (62)—to the active sample (63). These polymers interact sterically with microtubules through excluded volume interaction, enhancing the microtubule alignment and triggering a transition from contractile to extensile dynamics (Fig. 4D and SI Appendix, Fig. S9). Progressively increasing the nematic aligning interaction by adding more colloidal rods converted a globally contractile phase first into an aster phase, then into a fully extensile phase (SI Appendix, Fig. S10 A-D). The critical concentration of colloidal rods needed to trigger the transition increased with motor cluster concentration (SI Appendix, Fig. S10E). Dual imaging of motor clusters and tubulin at the single microtubule scale revealed that adding PEG, PRC1, or fd viruses did not prevent cap formation on isolated microtubules (Fig. 4 E-H). The fact that increasing depletion, cross-linking, and excluded volume interactions have the same effect on the transition argues that the impact of nematic alignment is generic. To summarize, our results demonstrate that the extensile-contractile transition arises from the competing effects of microtubule end-clustering, which favors the formation of contractile asters, and factors promoting microtubule alignment, which favors the formation of extensile bundles (Fig. 5A).

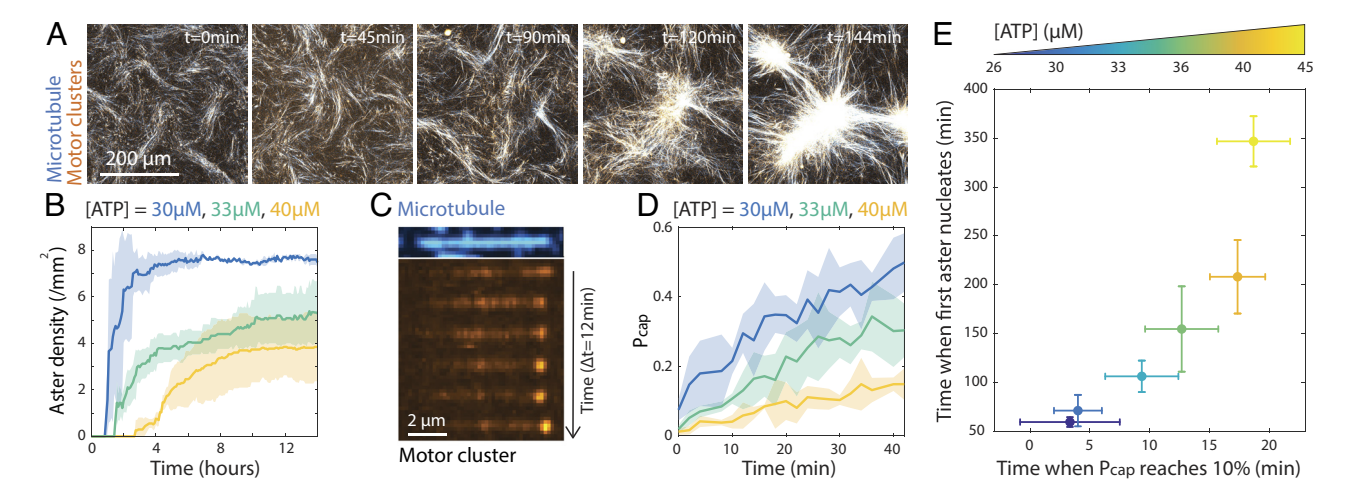


Fig. 3. Dynamics of aster formation correlates with dynamics of motor cap formation. (A) Time-series of the aster nucleation. Asters nucleate in an extensile background around 2 h after the start of the experiment. Tubulin is labeled in cyan, and motor clusters are in orange. [ATP] = 33 µM, [motor cluster] = 200 nM, [PEG] = 0.6% (vol/vol). (B) Temporal evolution of aster density for samples with increasing ATP concentrations. Asters nucleate more slowly with more ATP. (C) Kymograph (space-time plot) of the formation of a motor cap at the end of a single microtubule. Microtubule is shown in cyan and motor clusters in orange. (D) Temporal evolution of P_{cap}, the fraction of microtubules with a motor cap, for samples with increasing ATP concentrations. Motor caps form more slowly with more ATP. (E) Plot of the time when the first aster nucleates vs. the time when 10% of the microtubules have a motor cap. The color code shows experiments at various ATP concentrations. (A and C) were taken with a confocal microscope. The scale bar in A is 200 µm. The scale bar in C is 2 µm. Each experiment in (B, D, and E) was repeated three times independently. Thick lines in (B and D) and the disks in (E) show mean values, while shaded areas and error bars show the SD over the three replicates.

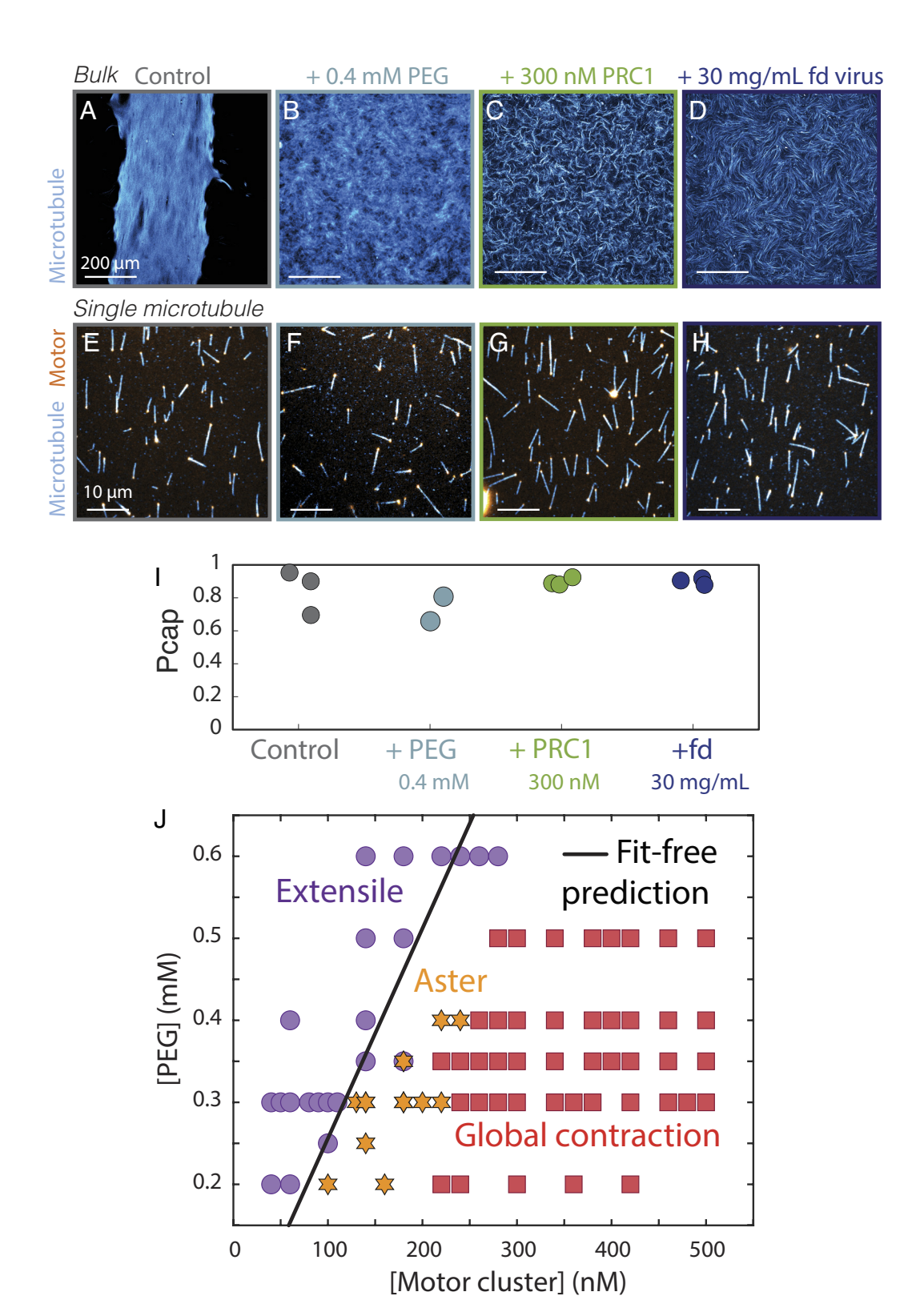


Fig. 4. Nematic alignment outcompetes polar sorting to drive a contractile-to-extensile transition, despite the formation of motor caps at the single microtubule level. (A) Fluorescent picture of an active cross-linked gel with PRC1 instead of PEG in the globally contractile phase ([ATP] = 30 μM, [Motor cluster] = 480 nM, [PRC1] = 100 nM, [Tubulin] = 1.33 mg/mL). Tubulin is labeled in cyan. (B) Adding 0.4 mM (0.8 % vol/vol) of 20 kDa PEG suppressed the global contraction and delayed the appearance of asters from an initially extensile phase by 1 h. Adding (C) 300 nM of PRC1, or (D) 30 mg/mL of fd virus to increase nematic alignment fully suppresses any contraction over the lifetime of the sample (4 h). Pictures in (A–D) were taken 1 h after dynamics started. (E–H) High-magnification microscopy of isolated microtubules for the same experimental conditions as in (A–D). Tubulin is labeled in cyan, and motor clusters are in orange. (I) Fractions of the microtubules with a motor cap for the same experimental conditions as (A–D). (I) A PEG-motor cluster phase diagram shows how the ratio of both components sets the extensile or contractile dynamics in active gels. Disks, stars, and squares represent experimental data, while the black line represents the no-fit prediction derived from the self-assembly model and the fitted parameters from the phase diagram in Fig. 1J. (A–H) were taken with a confocal microscope. The scale bar in (A–D) was performed three times independently except the one where PEG was added which was performed two times. Each data point shown in (J) comes from an independent experiment.

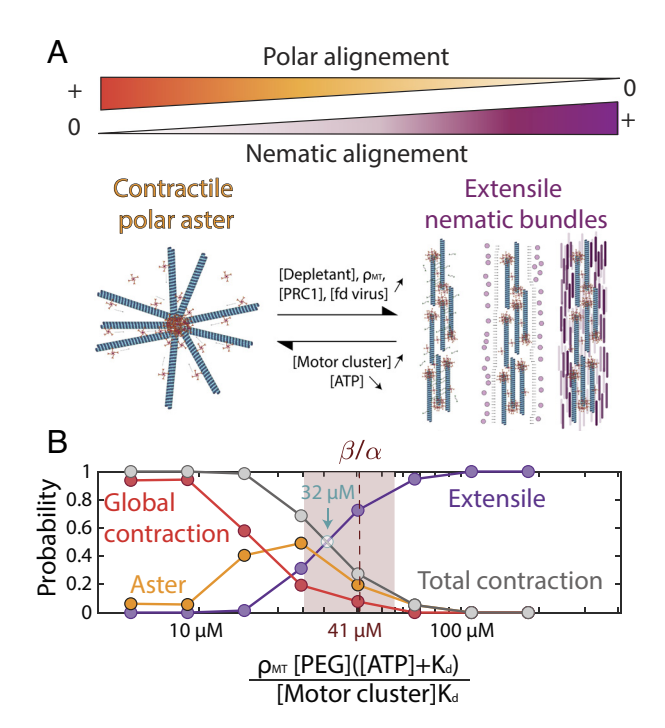


Fig. 5. Nematic alignment competes with polar sorting to control the self-assembly into extensile bundles or contractile asters. (A) Schematic representation of a contractile aster composed of polarity-sorted microtubules. Increasing the strength of nematic alignment by increasing the concentration of depletant, microtubule, PRC1 cross-linker, or fd virus can trigger a structural transition from contractile aster to extensile bundles. Decreasing the concentration of motor cluster or increasing the concentration of ATP decreases the probability of cap formation, which decreases the strength of polar end-adhesion interactions. At the macroscale, this leads to a transition from contractile asters to extensile bundles. (B) Relative probability of finding the active gel in the extensile, aster, or globally contractile phases as the rescaled concentration $\frac{p_{MT}[PEG][(ATP] + K_d)}{[Motor\ cluster_{tot}]K_d}$ increases. Disks show experimental data points. The raw 2D phase diagrams are shown in Figs. 1J and 4J and *SI Appendix*, Fig. S13. Above a critical microtubule density ($c^* = \beta / \alpha$), the active gel evolves on average from a contractile to extensile phase. The experimental estimate of c^* where extensile and contractile phases are equiprobable is 32 μ M. The dashed line shows the fitted value for $c^* = 41 \mu$ M, and the brown area shows the corresponding interval of 95% confidence for \emph{c}^{*} (25 to 56 $\mu\text{M}). Both$ are estimated by fitting the phase diagram in Fig. 1J. In B, N = 311 independent experiments, for [ATP] = 20 to 150 μ M, [Motor cluster] = 40 to 500 nM, [PEG] = 0.2 to 0.6 mM, i.e., 0.4 to 1.2%/% vol, [MT] = 2.7 to 16 nM.

Next, we developed a minimal steady-state model to rationalize the transition from extensile bundles to contractile asters. We took a self-assembly approach where polar and nematic interactions compete to dictate the steady-state structure of the kinesin-microtubule network. Polar interactions depend on the ability of the motor clusters to end-accumulate. If these multivalent clusters form a motor cap on a microtubule, they will naturally recruit other microtubules that will end-accumulate. These end-bound microtubules are free to splay but cannot slide and hence will form an aster (30, 42). Nematic interactions depend on the ability of the microtubules to stay aligned. In this state, the microtubules are free to slide but cannot splay and hence will form an extensile bundle.

Using the well-known depletion interaction (64, 65), we modeled the effective strength of the alignment interaction between two microtubules as:

$$V_{\text{alignment}} = \alpha L[PEG] \rho_{MT}^2,$$
 [1]

where α is a proportionality constant, L is the average microtubule length, [PEG] is the concentration of PEG in the system, and ρ_{MT} is the number density of microtubules. The quadratic scaling for ρ_{MT} results from the pairwise interaction between microtubules.

Similarly, we modeled the effective strength of the end-adhesion interaction as:

$$\begin{split} V_{\text{end-adhesion}} &= \beta L \frac{[Motor\ cluster_{ADP}]}{\rho_{MT}} \rho_{MT}^2 \\ &= \beta L [Motor\ cluster_{ADP}] \rho_{MT}, \end{split} \tag{2}$$

where β is a proportionality constant, and $\frac{[\textit{Motor cluster}_{\textit{ADP}}]}{\rho_{\textit{MT}}}$ is

the number of nonmotile, ADP-bound motor clusters per microtubule. In this model, the number of bound motors increases linearly with microtubule length, and thus, the strength of end-adhesion interaction increases linearly with L. This scaling is motivated by the experimental observation that the probability of having a motor cap increases with microtubule length, which is reminiscent of an antenna model (32, 53) (SI Appendix, Fig. S3G). As the run length of the motor clusters was larger than the microtubule length (SI Appendix, Fig. S5), we estimated that all motors bound to microtubules walk toward the microtubules' end and therefore only contribute to the end-adhesion interaction. Further, we considered that only ADP-bound motors that are attached at the end of a microtubule contribute to the end-adhesion. Considering an alternative model where ATP-bound motor clusters contribute to end-adhesion was incompatible with experimental measurements (SI Appendix, Fig. S11 and section 5). We further assumed that the binding of ATP to the motor clusters follows a simple binding equilibrium characterized by a dissociation constant K_d . The concentration of ADP-bound clusters is given by:

$$[Motor\ cluster_{ADP}] = [Motor\ cluster_{tot}] \left(\frac{K_d}{K_d + [ATP]}\right), [3]$$

where [Motor cluster_{tot}] is the total concentration of motor clusters, and K_d is the dissociation constant for ATP binding to the motor clusters (i.e., the concentration of ATP where half of the motors have ATP bound).

In this framework, the phase boundary between the bundle and aster phases should lie where the nematic alignment interaction strength (Eq. 1) equals the polar end-adhesion interaction strength (Eq. 2), providing the following prediction for the phase boundary in the ATP-motor cluster plane:

$$[ATP] = \frac{\beta K_d}{\alpha \rho_{MT} [PEG]} [Motor\ cluster_{tot}] - K_d.$$
 [4]

The experimental phase boundary separating the extensile bundle phase from the contractile aster phase in the ATP-motor cluster plane was linear in the range of concentrations explored (Fig. 1/), in agreement with the model. Fitting the experimental phase boundary to the model prediction (Eq. 4), provided estimates of the model parameters

$$\frac{\beta K_d}{\alpha \rho_{MT}[PEG]} = 376 \pm 147 \text{ and}$$

$$K_d = 14.5 \pm 25 \,\mu\text{M (fit values} \pm 95\% \,\text{CIs)}.$$

This measured value for the dissociation constant is lower than reported values for the same K401 construct, albeit under different experimental conditions ($K_d = 96.4 \pm 25 \mu M$ (66)). We independently estimated $K_d = 75 \pm 12 \,\mu\text{M}$ by measuring how the steady state speed of extensile gels varies with ATP concentration (SI Appendix, Fig. S12 and section 4c). Further work is needed to understand why the effective K_d derived from fitting the model differed from independent measurements.

Furthermore, the model predicts that the phase boundary in the PEG-motor clusters phase diagram is linear, and the previously measured fit parameters set the boundary's slope. We overlaid the fit-free prediction for the phase boundary with the experimental data points and found excellent agreement between experiments and theory (Fig. 4)). Finally, the model predicts that the slope of the phase boundary in the ATP-motor cluster plane scales inversely with the microtubule density, which was consistent with experimental observations that increasing microtubule number density induced a transition from contractile asters to extensile bundles in PEG-based active gels (SI Appendix, Fig. S4A).

This self-assembly framework can be modified to account for aligning interactions produced by the microtubule-specific cross-linker PRC1 instead of the depleting agent PEG. We modeled the effective strength of the alignment interaction between two microtubules as:

$$V_{\text{Alignment}} = \alpha L \frac{[PRC1]}{\rho_{MT}} \rho_{MT}^2 = \alpha L [PRC1] \rho_{MT},$$
 [5]

where the number of cross-linkers per microtubule [PRC1] / ρ_{MT} replaces the concentration of PEG as PRC1 needs to bind to a microtubule to induce alignment, while PEG does not. The theory predicts that the new phase boundary in the ATP-motor cluster plane is now independent of the density of microtubules ρ_{MT} :

$$[ATP] = \frac{\beta K_d}{\alpha [PRC1]} [Motor \ cluster_{tot}] - K_d.$$
 [6]

We assembled PRC1-based active microtubule gels in a contractile phase and systematically increased the number density of microtubules from 0.33 mg/mL to 10 mg/mL (SI Appendix, Fig. S4 B and C). We found that the emergent dynamics were always contractile in that range of concentrations, consistent with Eq. 6. Therefore, while both PRC1 and PEG induce nematic alignment of microtubules, this minimal model accounts for the different ways they interact with microtubules, explaining their distinctive impact on the self-assembly of microtubule-based active gels.

Despite the initial complexity of the five-dimensional organization phase space—ATP, motor clusters and PEG concentrations, microtubule number density, and microtubule length—this model provides a simple design rule to assemble active microtubule gels in targeted configurations. In this framework, a single control parameter given by the ratio of K_d and the various component concentrations: $\frac{\rho_{MT}[PEG]([ATP] + K_d)}{[Motor\ cluster_{tot}]K_d}$ dictates the self-assembly of the emergent structures in PEG-based active gels. Estimating ρ_{MT} from the known tubulin concentration, the number of protofilaments in a microtubule, and the measured length distribution, we rescaled all the experimental data points from ~300 independent experiments (SI Appendix, Fig. S13) onto a single 1D phase diagram. We computed the probability of being in a globally contractile, aster, or extensile phase as the ratio $\frac{\rho_{MT}[\text{PEG}]([ATP] + K_d)}{[Motor\ cluster_{tot}]K_d}$ increased (Fig. 5B). The model predicts that the phase boundary between the extensile and aster phase is set by the critical number density $\beta/\alpha = 41 \pm 15 \,\mu\text{M}$ (95% Confidence Intervale on linear fit). Below this critical density, our model predicts that microtubules will form asters, while above they will form bundles. We find that the number density c^* where extensile and contractile

phases are equiprobable lies within the 95% CI of the fitted value

for β/α ($c^* = 41 \mu M$, Fig. 5B). Excellent agreement between theory and experiments suggests that a self-assembly process governed by the competition between polar and nematic alignment interactions describes the extensile-to-contractile transition (Fig. 5A).

Discussion

To summarize, we bridged the length scale gap between the molecular interactions and the emergent macroscopic structure, explaining the transition from extensile bundles to contractile asters in active gels composed of stabilized microtubules, multivalent clusters of kinesin-1 motors, and either a depletant or microtubulespecific cross-linkers. We identified kinetics of motor-microtubule interactions that lead to either uniform motor distribution along microtubules or the end-accumulation of motors, which relate in part to the emergence of extensile bundles or contractile asters. We show that the dynamics of end-accumulation at the single filament scale sets the macroscopic emergent timescale of aster formation. Further, we show that end-clustering is insufficient to explain fully the extensile-to-contractile transition. Nematic interactions driven by depletion, cross-linking, or excluded volume interactions can outcompete polar sorting to favor extensile bundles over polarity-sorted contractile asters, even in conditions where motor clusters end-accumulate. A minimal self-assembly model based on the competition between microtubule endclustering driven by end-accumulated motors and nematic alignment captures the experimental trends. We further verified predictions of the model that differentiated between depletant and cross-linker-based active gels and demonstrated that a single control parameter given by the ratio of the concentrations of the components sets the structural transition from extensile bundles to contractile asters.

We consider these findings in the context of previously published results on the extensile-to-contractile transition in cytoskeletal active gels. First, while previous work on kinesinmicrotubule gels focused on the role of side binding vs. endbinding motors (43), direct observation of both the bulk organization and motor cluster distribution on single microtubules reveals that nematic bundles can arise even when motors efficiently end-accumulate.

Second, several mechanisms have been proposed to account for the extensile or contractile nature of biomimetic active matter. Recent theoretical work proposed that nonlinear elasticity can rectify the activity of an extensile dipole, leading to bulk contraction (67-69). For actomyosin gels, nonlinearities in actin filament mechanics have been put forward as one mechanism leading to contraction. While similar emergent mechanical properties have been suggested in viscoelastic gels composed of kinesin-microtubules bundles dispersed in a passive actin network (18), our multiscale approach favors that the asymmetric distribution of motors leads to aster formation in kinesin-microtubule-based active gels. Our work highlights that protein-protein interaction kinetics plays a crucial role in setting the macroscale emergent dynamics.

Third, our work investigates how the contractile-to-extensile transition is impacted by crowding, microtubule density, and microtubule length, all of which were recently explored in computer simulations of kinesin-microtubule networks (70). One main difference between the two studies is that our microtubules are short compared to the motor clusters' run length (respectively 1.6 µm and 5.7 µm, SI Appendix, Fig. S5) while the simulated microtubules range from 2.5 to 15 µm. Our results confirm that crowding promotes extensile bundles over contractile asters, and we report additional results regarding the impact of microtubule length and their number density when microtubules are shorter than the motor clusters' run length: Increasing microtubule density leads to extensile bundles in PEG-based networks, and increasing microtubule length does not impact the transition. In this regime, longer microtubules favor nematic alignment and end-accumulation equally because of the antenna effect. When microtubules are longer than the run length, our model predicts that increasing microtubule length would only enhance the alignment interaction, leading to a transition from contractile asters to extensile bundles, thus corroborating the results of the computer simulations for long microtubules (70).

Our results are also consistent with how microtubule networks powered by end-accumulating kinesin-4 motors self-organize in the presence of a depletant (34): Increasing microtubule number density and increasing PEG concentration both lead to a transition from contractile to extensile. Further, no extensile dynamics were observed in the absence of PEG, and increasing microtubule concentration induced a contractile-to-extensile transition in the presence of PEG for both motor constructs. However, contrary to our results for kinesin-1 clusters, the transition for kinesin-4 is independent of the motor concentration, probably because the motor protein always end-accumulates. We did not explore the experimental regime where an active foam phase is observed with kinesin-4 motors.

Finally, while depletant has been a long-time favorite bundler for microtubule-based active gels (4), PRC1 cross-linkers have recently been used to assemble extensile active gels (6, 71, 72) and active composite materials (18, 63). Our work highlights the similarities and differences of how depletants and cross-linkers impact the self-organization of microtubule-based active gels.

This work illustrates how to leverage simple concepts from self-assembly to understand complex emergent structures and dynamics in an out-of-equilibrium material powered by chemical reactions. One important takeaway of the theory is that asters nucleation and polarity sorting are not the consequence but rather the cause of local contractility. However, it is unclear why this minimal steady-state model captures the extensile-to-contractile transition so well (Fig. 5B). Indeed, this mean-field theory only considers pairwise interactions and lacks any higher-order cooperativity between microtubules, or between microtubules and motor clusters (33, 73, 74). Second, this theory has no intrinsic timescales, hence no dependence on reaction rates which are crucial for explaining the interactions between kinesin and microtubules. Third, this model cannot describe the scale-dependent architecture of the active gels. When end-adhesion dominates, microtubules with motor caps are predicted to form micelle-like structures with a radius of one microtubule length (34). However, the aster sizes observed here are orders of magnitude larger than the average microtubule length, which clearly shows that the model cannot give information about the hierarchical organization that leads to the observed mesoscale structures (Fig. 1 *H* and *I*). Consequently, this model does not describe the percolation transition from asters to globally contractile gels (75). Finally, we expect that the critical ratio delineating the extensile and contractile phases will be different for different motors, cluster valency, or buffer conditions (Fig. 5B). One piece of evidence is that adding salt eliminates any contraction without changing protein composition (SI Appendix, Fig. S6).

These results further highlight that motor clusters' valency and processivity dictate, in part, the self-organization of the active gel at the macroscale. Processivity is required to drive end-accumulation (32) and aster formation. No contraction had been observed with light-activated K365 dimers as they are nonprocessive by design (SI Appendix, Fig. S7). In contrast, the other constructs potentially form asters because the motor clusters are multivalent, hence highly processive (40), and readily able to end-accumulate. These results underscore the importance of paying close attention to the design of the motor cluster, as they significantly impact the self-organization of the cytoskeletal active gels.

Taken together, this work offers a blueprint for the predictive assembly of cytoskeletal active matter, particularly for building multifunctional active materials that can be programmed into distinct or coexisting far-from-equilibrium structures.

Data, Materials, and Software Availability. All study data are included in the article and/or supporting information.

ACKNOWLEDGMENTS. We thank Shibani Dalal, director of the Brandeis Biomaterial Facility, for help with protein purification. B.N. thanks Saptorshi Ghosh for the discussion on data analysis. We thank Daichi Hayakawa for providing six helix bundle DNA origami rods and Salman Alam for providing the fd viruses. We thank Linea Lemma for the opto-K365 constructs and Bennett Sessa for comments on the manuscript. B.N. thanks Ian Murphy for helping with the native gel electrophoresis. We thank Seth Fraden for helping interpret the Dynamic Light Scattering and the native gel results. B.N. and G.D. acknowledge support from the NSF CAREER award DMR-2047119. P.J.F. and A.B. acknowledge support from the Brandeis NSF Materials Research Science and Engineering Center (MRSEC) DMR-2011846. We also acknowledge the use of the optical, microfluidics, light scattering, and biomaterial facilities supported by NSF MRSEC DMR-2011846. A.B. acknowledges support from NSF-DMR-2202353.

Author affiliations: ^aDepartment of Physics, Brandeis University, Waltham, MA 02453

- M. C. Marchetti et al., Hydrodynamics of soft active matter. Rev. Modern Phys. 85, 1143 (2013).
- W. B. Rogers, W. M. Shih, V. N. Manoharan, Using DNA to program the self-assembly of colloidal nanoparticles and microparticles. *Nat. Rev. Mater.* **1**, 16008 (2016).
- L. Wurthner et al., Bridging scales in a multiscale pattern-forming system. Proc. Natl. Acad. Sci. U.S.A. 119, e2206888119 (2022).
- T. Sanchez, D. T. Chen, S. J. DeCamp, M. Heymann, Z. Dogic, Spontaneous motion in hierarchically assembled active matter. *Nature* **491**, 431–434 (2012).
- N. Kumar, R. Zhang, J. J. de Pablo, M. L. Gardel, Tunable structure and dynamics of active liquid crystals. Sci. Adv. 4, eaat7779 (2018).
- P. Chandrakar et al., Confinement controls the bend instability of three-dimensional active liquid crystals. Phys. Rev. Lett. 125, 257801 (2020).
- F. J. Nedelec, T. Surrey, A. C. Maggs, S. Leibler, Self-organization of microtubules and motors. Nature 389, 305-308 (1997).
- F. Backouche, L. Haviv, D. Groswasser, A. Bernheim-Groswasser, Active gels: Dynamics of patterning and self-organization. Phys. Biol. 3, 264-273 (2006).
- D. Smith et al., Molecular motor-induced instabilities and cross linkers determine biopolymer organization. Biophys. J. 93, 4445-4452 (2007).
- P. M. Bendix et al., A quantitative analysis of contractility in active cytoskeletal protein networks. Biophys. J. 94, 3126-3136 (2008).
- 11. M. P. Murrell, M. L. Gardel, F-actin buckling coordinates contractility and severing in a biomimetic actomyosin cortex. Proc. Natl. Acad. Sci. U.S.A. 109, 20820-20825 (2012).

- 12. P. J. Foster, S. Furthauer, M. J. Shelley, D. J. Needleman, Active contraction of microtubule networks. Elife 4, e10837 (2015).
- 13. I. Linsmeier et al., Disordered actomyosin networks are sufficient to produce cooperative and telescopic contractility. *Nat. Commun.* **7**, 12615 (2016).
- 14. T. H. Tan et al., Self-organized stress patterns drive state transitions in actin cortices. Sci. Adv. 4, eaar2847 (2018).
- 15. T. D. Ross *et al.*, Controlling organization and forces in active matter through optically defined boundaries. Nature 572, 224-229 (2019).
- V. Wollrab et al., Polarity sorting drives remodeling of actin-myosin networks. J. Cell Sci. 132, ics219717 (2018).
- 17. R. A. Banks et al., Motor processivity and speed determine structure and dynamics of microtubulemotor assemblies. eLife 12, e79402 (2023).
- 18. J. Berezney, B. L. Goode, S. Fraden, Z. Dogic, Extensile to contractile transition in active microtubuleactin composites generates layered asters with programmable lifetimes. Proc. Natl. Acad. Sci. U.S.A. 119, e2115895119 (2022).
- 19. N. Kumar, R. Zhang, J. J. de Pablo, M. L. Gardel, Tunable structure and dynamics of active liquid crystals. Sci. Adv. 4, eaat7779 (2018).
- R. Zhang et al., Spatiotemporal control of liquid crystal structure and dynamics through activity patterning. Nat. Mater. 20, 875-882 (2021).
- T. Gao, R. Blackwell, M. A. Glaser, M. D. Betterton, M. J. Shelley, Multiscale polar theory of microtubule and motor-protein assemblies. Phys. Rev. Lett. 114, 048101 (2015).

- 22. A. Lamtyugina, Y. Qiu, E. Fodor, A. R. Dinner, S. Vaikuntanathan, Thermodynamic control of activity patterns in cytoskeletal networks. Phys. Rev. Lett. 129, 128002 (2022).
- R. Blackwell et al., Microscopic origins of anisotropic active stress in motor-driven nematic liquid crystals. Soft Matter 12, 2676-2687 (2016).
- M. Lenz, Geometrical origins of contractility in disordered actomyosin networks. Phys. Rev. X 4,
- S. Stam et al., Filament rigidity and connectivity tune the deformation modes of active biopolymer 25. networks. Proc. Natl. Acad. Sci. U.S.A. 114, E10037-E10045 (2017).
- M. Murrell, P. W. Oakes, M. Lenz, M. L. Gardel, Forcing cells into shape: The mechanics of actomyosin contractility. Nat. Rev. Mol. Cell Biol. 16, 486-498 (2015).
- D. V. Koster et al., Actomyosin dynamics drive local membrane component organization in an in vitro active composite layer. Proc. Natl. Acad. Sci. U.S.A. 113, E1645-E1654 (2016).
- P. J. Foster, S. Fürthauer, N. Fakhri, Active mechanics of sea star oocytes. bioRxiv [Preprint] (2022). https://doi.org/10.1101/2022.04.22.489189.
- K. Kruse, F. Jülicher, Actively contracting bundles of polar filaments. Phys. Rev. Lett. 85, 1778 29 (2000).
- J. M. Belmonte, M. Leptin, F. Nedelec, A theory that predicts behaviors of disordered cytoskeletal 30 networks. Mol. Syst. Biol. 13, 941 (2017).
- R. Tan, P. J. Foster, D. J. Needleman, R. J. McKenney, Cooperative accumulation of dynein-dynactin at microtubule minus-ends drives microtubule network reorganization. Dev. Cell 44, 233-247.e4
- C. Leduc et al., Molecular crowding creates traffic jams of kinesin motors on microtubules. Proc. Natl. Acad. Sci. U.S.A. 109, 6100-6105 (2012).
- S. S. Wijeratne, S. A. Fiorenza, A. E. Neary, R. Subramanian, M. D. Betterton, Motor guidance by long-range communication on the microtubule highway. Proc. Natl. Acad. Sci. U.S.A. 119, e2120193119 (2022).
- B. Lemma, N. P. Mitchell, R. Subramanian, D. J. Needleman, Z. Dogic, Active microphase separation in mixtures of microtubules and tip-accumulating molecular motors. Phys. Rev. X 12, 031006 (2022).
- R. D. Vale et al., Direct observation of single kinesin molecules moving along microtubules. Nature 380, 451-453 (1996).
- A. Seitz, T. Surrey, Processive movement of single kinesins on crowded microtubules visualized using quantum dots. EMBO J. 25, 267-277 (2006).
- A. Parmeggiani, T. Franosch, E. Frey, Phase coexistence in driven one-dimensional transport. Phys. Rev. Lett. 90, 086601 (2003).
- W. O. Hancock, J. Howard, Kinesin's processivity results from mechanical and chemical coordination between the ATP hydrolysis cycles of the two motor domains. Proc. Natl. Acad. Sci. U.S.A. 96, 13147-13152 (1999).
- M. J. Schnitzer, S. M. Block, Kinesin hydrolyses one ATP per 8-nm step. Nature 388, 386-390
- K. Furuta et al., Measuring collective transport by defined numbers of processive and nonprocessive kinesin motors. *Proc. Natl. Acad. Sci. U.S.A.* 110, 501–506 (2013).
- K. Laki, W. R. Carroll, Size of the myosin molecule. Nature 175, 389-390 (1955).
- 42. W. Yan et al., Toward the cellular-scale simulation of motor-driven cytoskeletal assemblies. Elife 11, e74160 (2022).
- J. Roostalu, J. Rickman, C. Thomas, F. Nedelec, T. Surrey, Determinants of polar versus nematic organization in networks of dynamic microtubules and mitotic motors. Cell 175, 796-808.e14 (2018).
- G. Henkin, W. X. Chew, F. Nedelec, T. Surrey, Cross-linker design determines microtubule network organization by opposing motors. *Proc. Natl. Acad. Sci. U.S.A.* **119**, e2206398119 (2022).
- G. Sarfati, A. Maitra, R. Voituriez, J. C. Galas, A. Estevez-Torres, Crosslinking and depletion determine spatial instabilities in cytoskeletal active matter. Soft Matter 18, 3793-3800 (2022).
- G. Henkin, S. J. DeCamp, D. T. Chen, T. Sanchez, Z. Dogic, Tunable dynamics of microtubule-based active isotropic gels. Philos. Trans. A: Math. Phys. Eng. Sci. 372, 20140142 (2014).
- L. M. Lemma et al., Multiscale microtubule dynamics in active nematics. Phys. Rev. Lett. 127, 148001 (2021).

- 48. Y. Fan, K.-T. Wu, S. A. Aghvami, S. Fraden, K. S. Breuer, Effects of confinement on the dynamics and correlation scales in kinesin-microtubule active fluids. Phys. Rev. E 104, 034601 (2021).
- T. Surrey, F. Nédélec, S. Leibler, E. Karsenti, Physical properties determining self-organization of motors and microtubules. Science 292, 1167-1171 (2001).
- F. Verde, J. M. Berrez, C. Antony, E. Karsenti, Taxol-induced microtubule asters in mitotic extracts of Xenopus eggs: Requirement for phosphorylated factors and cytoplasmic dynein. J. Cell Biol. 112, 1177-1187 (1991).
- K. E. Sawin, K. LeGuellec, M. Philippe, T. J. Mitchison, Mitotic spindle organization by a plus-enddirected microtubule motor. Nature 359, 540-543 (1992).
- T. Gaglio, A. Saredi, D. A. Compton, NuMA is required for the organization of microtubules into asterlike mitotic arrays. J. Cell Biol. 131, 693-708 (1995).
- $L.\ Mohapatra,\ B.\ L.\ Goode,\ P.\ Jelenkovic,\ R.\ Phillips,\ J.\ Kondev,\ Design\ principles\ of\ length\ control\ of\ principles\ of\ princip\ of\ principles$ cytoskeletal structures. Annu. Rev. Biophys. 45, 85-116 (2016).
- L. M. Lemma et al., Spatiotemporal patterning of extensile active stresses in microtubule-based active fluids. PNAS Nexus 2, pgad130 (2023).
- E. C. Young, H. K. Mahtani, J. Gelles, One-headed kinesin derivatives move by a nonprocessive, low-duty ratio mechanism unlike that of two-headed kinesin. Biochemistry 37, 3467-3479 (1998)
- G. Guntas et al., Engineering an improved light-induced dimer (iLID) for controlling the localization and activity of signaling proteins. Proc. Natl. Acad. Sci. U.S.A. 112, 112-117 (2015).
- D. J. Needleman et al., Synchrotron X-ray diffraction study of microtubules buckling and bundling under osmotic stress: A probe of interprotofilament interactions. Phys. Rev. Lett. 93, 198104 (2004).
- M. Braun et al., Adaptive braking by Ase1 prevents overlapping microtubules from sliding completely apart. Nat. Cell Biol. 13, 1259-1264 (2011).
- Z. Lansky et al., Diffusible crosslinkers generate directed forces in microtubule networks. Cell 160, 1159-1168 (2015).
- $R.\ Subramanian\ \textit{et al.,}\ Insights\ into\ antiparallel\ microtubule\ crosslinking\ by\ PRC1,\ a\ conserved$ nonmotor microtubule binding protein. *Cell* **142**, 433–443 (2010).

 Z. Dogic, S. Fraden, Cholesteric phase in virus suspensions. *Langmuir* **16**, 7820–7824 (2000).
- M. Siavashpouri et al., Molecular engineering of chiral colloidal liquid crystals using DNA origami. Nat. Mater. 16, 849-856 (2017).
- G. Duclos et al., Topological structure and dynamics of three-dimensional active nematics. Science 367, 1120-1124 (2020).
- S. Asakura, F. Oosawa, On interaction between two bodies immersed in a solution of macromolecules. J. Chem. Phys. 22, 1255-1256 (1954).
- S. Asakura, F. Oosawa, Interactions between particles suspended in solutions of macromolecules. J. Polymer Sci. **33**, 183-192 (1958).
- K. M. Brendza, D. J. Rose, S. P. Gilbert, W. M. Saxton, Lethal kinesin mutations reveal amino acids important for ATPase activation and structural coupling. J. Biol. Chem. 274, 31506-31514 (1999).
- P. Ronceray, C. P. Broedersz, M. Lenz, Fiber networks amplify active stress. Proc. Natl. Acad. Sci. U.S.A. **113**, 2827-2832 (2016).
- M. Lenz, Reversal of contractility as a signature of self-organization in cytoskeletal bundles. Elife 9, e51751 (2020).
- F. Benoist, G. Saggiorato, M. Lenz, Generic stress rectification in nonlinear elastic media. Soft Matter **19**, 2970-2976 (2023).
- W.-X. Chew, G. Henkin, F. Nédélec, T. Surrey, Effects of microtubule length and crowding on active microtubule network organization. iScience 26, 106063 (2023).
- P. Chandrakar et al., Engineering stability, longevity, and miscibility of microtubule-based active fluids. Soft Matter 18, 1825-1835 (2022).
- B. Najma et al., Competing instabilities reveal how to rationally design and control active crosslinked gels. Nat. Commun. 13, 6465 (2022).
- A. Vilfan et al., Dynamics and cooperativity of microtubule decoration by the motor protein kinesin. J. Mol. Biol. 312, 1011-1026 (2001).
- W. H. Roos et al., Dynamic kinesin-1 clustering on microtubules due to mutually attractive interactions. Phys. Biol. 5, 046004 (2008).
- J. Alvarado, M. Sheinman, A. Sharma, F. C. MacKintosh, G. H. Koenderink, Molecular motors robustly drive active gels to a critically connected state. Nat. Phys. 9, 591–597 (2013).